Global Medical Genetics 12 (2025) 100001

Contents lists available at ScienceDirect

Global Medical Genetics

journal homepage: www.keaipublishing.com/en/journals/gmg/

The pathogenesis of B-cell non-hodgkin lymphoma associated with HBV (hepatitis B virus) infection is regulated by c-Myc/PD-L1 signaling pathway

Yu Zhao[a,1], Jian Yang[b,1], Sai Xu[a,1], Ying Wang[b,*], Jian Bo[a,**]

[a] Senior Department of Hematology, The Fifth Medical Center of Chinese PLA General Hospital, No 8 East Street, Fengtai District, Beijing 100071, China
[b] Clinic of Yongding Road, Southern Medical Branch of PLA General Hospital, No 27 Taiping Road, Haidian District, Beijing 100036, China

ARTICLE INFO

Keywords:
B-NHL (B cell non-Hodgkin's lymphoma)
HBV (Hepatitis B virus)
C-Myc
PD-L1
Transcriptome
Circulating tumor cell (CTC)

ABSTRACT

Background: HBV is closely associated with the incidence of B-NHL (B-cell non-hodgkin lymphoma). This project intends to establish HBV infection-induced B-NHL cells and animal models to clarify the mutual mechanism of HBV infection and B-NHL pathogenesis.
Methods: The relationship between HBV and B-NHL was studied based on the HBV infection model, which included CTC cells and HBV transgenic mice. Moreover, differential expression analysis of transcriptome profiling was performed to confirm the mechanism.
Results: The HBsAg expression and HBV-DNA could be found in tumor tissues of HBV group, but negative in the control group. Moreover, there were clearly differences between the two groups in the transcriptome of tumor tissues and CTC. HBsAg significantly promoted lymphocytes associated with c-Myc and PD-L1.
Conclusion: The promoted effect induced by HBsAg in lymphocytes was associated with PD-L1 mediated by c-Myc.

Introduction

Lymphoma is rapidly increasing in the world, 90 % of which are NHL (Non-Hodgkin's lymphoma), and causes great harm to human health, and its prognosis is extremely poor [1]. In addition, lymphoma is the hematological malignant tumor with the fastest growing incidence [2]. NHL causes approximately 360,000 patients to die every year after failure of systemic treatment. The incidence of malignant lymphoma is about 3.5 per 100,000, with approximately 84,000 new patients and more than 20,000 deaths each year, showing a significant rapid increase [3]. Lymphoma occupies the 9th place among the ten most common malignant tumors in men and the 10th place among women [4].

There are many types of lymphomas and their pathogenesis is complicated. Moreover, germinal center (Germinal center) origin lymphoma accounts for 80 % of NHL, including diffuse large B lymphoma, follicular lymphoma, and Burkitt lymphoma [5]. The

* Corresponding author.
** Correspondence to: Department of Hematology, Fifth Medical Center, Chinese PLA General Hospital, No. 28 Fuxing Road, Haidian District, Beijing 100853, China.
E-mail addresses: 13911517672@139.com (Y. Wang), boj301@sina.com (J. Bo).
[1] These authors are contributed equally to this work.

https://doi.org/10.1016/j.gmg.2024.100001

feature of pathogenesis is that B cells go through different stages of the germinal center, gene mutation translocation occurs [6]. The main causes of lymphoma include viral and/or bacterial infections, immune disorders, occupational, and environmental factors [7].

Studies have confirmed that people infected with HBV (Hepatitis B virus) have a significantly higher risk of developing NHL [8–11]. Zhou et al. analyzed the case data of more than 600,000 patients who participated in cancer prevention research, of which about 53,000 patients were HBV DNA positive. The proportion of NHL in those cases with HBV infection is about 19.4 per 100,000 after 14 years, while the proportion of NHL in those patients who are not infected with HBV is about 12.3 per 100,000, it indicates the significant statistical difference [12]. In addition, some scholars used the meta-analysis method to conduct research and found that the OR value and 95 % CI of HBV infection were 1.59 (1.06–2.37), respectively. It suggested that HBV infection is one of the risk factors for the occurrence of malignant lymphoma [13]. However, the reason the incidence of lymphoma has increased year by year is not clear, but it is closely related to certain special viruses and bacterial infections, especially in HBV infection or carrier diseases. Moreover, the risk of non-Hodgkin's lymphoma, especially B-cell lymphoma, is higher than that of ordinary people for 2–3 times [14]. The previous research of our group has found that in the tumor tissues of HBsAg-positive patients with B-NHL, HBsAg expression could be detected based on immunohistochemistry analysis, meanwhile HBV-DNA was positive according to situ hybridization. Additionally, HBsAg protein can significantly upregulate c-Myc and PD-L1 expression levesl in normal human B lymph nodes, and promote cell proliferation.

Therefore, this project intended to establish the cell and animal model of B-NHL caused by HBV infection to clarify the interaction between the HBV infection process and the pathogenesis of B-NHL. Furthermore, our work explored and determined that HBsAg protein was regulated by c-Myc during the process of B-NHL caused by HBV infection associated with PD-L1 signaling pathway.

Materials and methods

Patients and samples

Seventy-seven patients with B-cell NHL were diagnosed in Chinese PLA General Hospital from January, 2010 to December, 2020. They were participated in the clinical trial. Of these individuals, there were forty-one patients with DLBCL (Diffuse large B-cell lymphoma), twelve patients with FL (Follicular lymphoma), seven patients with BL (Burkitt Lymphoma), six patients with HGBL (High Grade B-cell Lymphomas), six patients with MCL (Mantle cell lymphoma), three patients with MZBL (Marginal zone B-cell lymphoma), two patients with MALT (Mucosa associated lymphoid tissue type). The pathological diagnosis was based on the 2016 WHO diagnostic criteria for lymphoma [15,16].

All patients' paraffin section tissue samples and peripheral blood samples were collected at the first visit before treatment. The thickness of the paraffin tissue section was 4 μm. Peripheral blood samples were collected with EDTA tubes, and then centrifuged to separate plasma within 4 h, stored in a refrigerator at −20 ℃.

The diagnosis and classification of lymphoma can be divided into stages from one to four stages. In the first stage, the disease only involves two lymph node areas, or a single extranodal organ is locally affected. In the second stage, the lesion involves two or more lymph node areas, and the lesions are limited to invading organs other than lymph nodes or more than one lymph node area. In the third stage, there are lymph node lesions above and below the diaphragm, which may be accompanied by involvement of the spleen, limited involvement of extranodal organs, or involvement of the spleen and limited extranodal organs. In the fourth stage, one or more extranodal organs may be extensively or disseminated, with or without lymphadenopathy, liver, or bone involvement, all belonging to the fourth stage. According to the symptoms, it can be divided into two groups: Group A and Group B. Group A has no symptoms, and patients in Group B are often accompanied by some symptoms of fever, night sweats, and general malaise.

Our works were ethically approved by the Ethics Committee of Chinese PLA General Hospital based on the Declaration of Helsinki. All participants signed the informed consent, and the ethical approval number was 0310–0064.

Immunohistochemical analysis

The tissues were sliced, which was baked at 60 ℃ for 1 h, then stepwisely dewaxing and rehydrating with xylene for 10 min, stepwise ethanol (100 %, 95 %, 90 %, 85 %, 80 %, 75 %, 60 %, 50 %, 30 %) for each 5 min, tap water for 1 min, and hydrogen peroxide for 1 min. Moreover, utilization of 30 % H_2O_2 plus 10 parts of distilled water for 10 min at room temperature, distilled water wash. The slices were immersed in 0.01 M citric acid buffer, heated to boiling in the microwave at the maximum power (98 ℃−100 ℃), cooled (about 5–10 min), and repeated twice for microwave repair. Naturally cooled the slices to room temperature and washed with PBS, then blocked with 5 % BSA for 20 min at room temperature, shake off excess liquid. Add primary antibody dropwise, 37 ℃, 1 h, or 4 ℃ overnight, wash with PBS. Furthermore, added secondary antibody dropwise at 37 ℃, washed with PBS. Added SABC dropwise, 37 ℃, washed with PBS and distilled water, respectively, then drop the color reagent, mix. After the color reagent of DAB was configured, added it onto the section at room temperature, and checked the reaction time under the microscope (about 5 min). Tap water and distilled water were used to rinse, respectively. Then hematoxylin counterstained for 2 min, rinsed with tap water. Dehydrate with stepwise ethanol (30 %, 50 %, 70 %, 80 %, 90 %, 95 %, 100 %) for each 3 min, consequently xylene 20 min. Finally, the gum enveloped microscopic examination.

Next generation sequencing

The isolated total RNA was assessed with agarose gel electrophoresis. RNA degradation and contamination were removed, then purified RNA was extracted with Thermo Scientific KingFisher Pure RNA Tissue Kit. Bioanalyzer 2100 system and Nano 6000 RNA

Assay Kit was used to assess the integrity of RNA. The RIN values of all samples were above eight. Then, separate Illumina sequencing libraries were generated and purified from pooled samples with TruSeq™ RNA Sample Preparation Kit. The synthesized first and second strand cDNA were ligated to adapter oligonucleotides. Moreover, AMPure XP system was used to purify and quantify the library fragments, then we obtained paired-end reads (0–100 bp).

Analyze bioinformation

The fastq clean data were obtained using raw, then the sequence and content duplication levels of GC, Q20, and Q30 were calculated. The workflow for complete RNA-seq is provided by Cufflinks and TopHat. Its core step is the alignment of sequencing data with the reference genome. The economical FM index bowtie is usually utilized for alignment 'engine', it stores the sequence of the reference genome and is the extreme data structure. The transcripts expressions were accurately quantified by alignment, gene discovery and transcript assembly were addressed to analyze differential expression. The linear statistical model is implemented to evaluate the assignment abundance by Cuffdiff and Cufflinks. Each transcript can explain the maximum likelihood of the observed reads. The individual transcripts were assembled from RNA-seq reads with cufflinks, which reported the transcriptome assembly data and aligned to genome. Moreover, the expression level was quantified in each transfrag of the sample with cufflinks after the assembly phase. Numerous output files were reported by Cuffdiff and contained differential analysis results. Besides, simple tabular output files reported the changes of transcript and gene expression level, which described the attribution of gene and transcript expression, including common locations and names in genome. Moreover, the differential analysis results about gene expression were identified by Cuffdiff, which also confirmed differentially regulation through promoter switching and differentially spliced genes. The differential regulation expression was conducted with Cuffdiff at gene and transcript level. CummeRbund was used to integrate, visualize, and manage all data coming from Cuffdiff analysis. The –mask/-M option was used to exclude gene Cufflinks. During differential analysis, these genes were added into the final transcriptome file by Cuffmerge based on the available reference transcriptome annotation.

Detection of CTC (Circulating tumor cells)

Sample preparation

Added 3 ml of normal saline to a 15 ml centrifuge tube, then fixed with 200 μl 8 % PFA and mixed with a Pasteur tube, took 5 ml blood sample from the blood collection tube and transferred it into the 15 ml centrifuge tube, the total volume was about 8 ml. Mixed by pipetting upside down with the Pasteur tube, and placed it at room temperature for 10 min, then transferred the sample to a prewashed filter, and performed whole blood separation in an abnormal cell separation staining instrument (not separate staining).

Filter membrane

Open the upper plug before taking the membrane, add 100 μl 0.4 % PFA to the filter and fixed at room temperature for 5 min. Opened the lower plug and allowed the PFA to flow out naturally. Dropped 2.5 μl of the patch tablet onto the glass slide, smeared it to the size of the filter membrane, used the membrane remover to remove the fixed filter membrane, putted the front side up on the slide glass, dried at room temperature for 3 min, and waited for the membrane to dry. After that, took the immunohistochemistry pen and drew a circle along the edge of the filter membrane. Rinsed with BD Perm/Wash buffer (diluted 1:10 in distilled H_2O) for 3 times, 3 min each time.

Fixation and perforation

The solution for Fixation and Permeabilization solution (BD) was used to dropwise, then placed the slide in a wet box, incubated at 4 ℃ for 20 min, rinsed with BD Perm/Wash buffer 3 times, 3 minutess each time.

Blocking

Added 100 μl 10 % Goat Serum dropwise to the filter membrane and blocked for 45 min at room temperature.

One antibody incubation

The primary antibodies Anti-c-Myc and Anti-PD-L1 were gently pipetted to the mix after preparation. Added dropwise to the filter membrane and incubated at 4 °C, overnight. After the incubation was completed, rinsed with BD Perm/Wash buffer 3 times for 3 min each time.

Secondary antibody incubation and nuclear staining

The goat Anti-mouse (488) or goat Anti-rat (546; Alexa Fluor) was used as secondary antibody, nuclear staining reagent was used Hochest.

Mounting and testing

GVA water-soluble mounting tablets were added dropwise to mount the slides, and the slides were examined under a fluorescence microscope.

Cell culture

The extracted CTC cells were cultured in DMEM medium contained with FBS.

The plasmid transfections

The shRNA plasmid of pSilencer2.1-neo vector was used to interfere with c-Myc expression, the RNAi targeting sequence for c-Myc was confirmed.

Western blot analysis

The protein electrophoreses were conducted on SDS-PAGE gel. Moreover, the blocked membrane transferred to proteins was sealed using skim milk, then probed with primary antibody. Antibodies were primarily utilized in our work: anti-β-actin (13E5) (Cell Signaling, Danvers, MA, USA; CST 4970S, dilution 1: 2000), anti-c-Myc (Abcam; ab 32072: dilution 1:2000), anti-PD-L1 (ab205921, 1:1000; Abcam, Cambridge, MA, USA). Finally, the chemiluminescence examination was performed based on the secondary HRP antibody using the exposed film.

Animals

One hundred twenty female mice, the FI generation of fathers carrying the hepatitis B virus surface antigen gene driven by the rat albumin promoter [17–19] and of normal C57BL/6 mothers, were produced at Scripps Clinic and Research Foundation and tested for the presence of the HBV transgene and for serological evidence of HBsAg, as previously described [19]. Groups of 20 aged matched female mice and their non-transgenic littermates were divided into subgroups (one subgroup containing the transgene and the other subgroup not containing the transgene) and shipped from Scripps to the Animal Care Unit at the Chinese PLA General Hospital in Beijing. All mice were individually identified according to the ear code prepared and were arbitrarily assigned to treatment groups. In this way, both subgroups A and B within groups 1–6 were exposed to the same regimen, without the investigators knowing which subgroup carried the HBsAg transgene. Animals were maintained in negative pressure-vented Plexiglas containment cabinets based on climate-controlled rooms with light-dark cycle (12-h) according to institutional animal welfare and biohazard review committee guidelines and received food and water ad libitum. Bleeding from the retro-orbital sinus and sacrifices were performed under ether anesthesia, according to procedures approved by the institutional animal welfare committee.

The xenograft mouse model

The nude mice obtained from the Laboratory Animal Center of Chinese PLA General Hospital (Beijing, China) was used to construct the xenograft mice model. This work was approved by the Ethical committee of Chinese PLA General Hospital. The CRC suspension was utilized to construct the tumor model as a common method. After sacrifice at 21th day, trial was performed for tumor mass, c-Myc, and PD-L1 expression in tumor tissues, respectively.

Statistics

The information was shown as mean ± Standard deviation (SD). Student's *t*-test was utilized to analyze the group differences. SPSS software (version 18.0) was utilized to perform these statistical analyses. $P < 0.05$ is significant statistically.

Results

B-NHL was associated with HBV infection

The case data and the corresponding serum or lymph node tissue samples of these patients were accumulated. The serum HBsAg levels and HBV-DNA were firstly determined. The serum level of HBsAg in all patients with B-NHL in HBV group (n = 41) were positive, but 48% of them had positive of HBV-DNA. On the contrary, B-NHL patients without HBV infection in the control group (n = 36) were negative for serum HBsAg and HBV-DNA levels. There was no statistical difference between the two groups in terms of demographic characteristics, lymphoma classification or staging, and recovery after treatment. Moreover, the immunohistochemical stain of HBsAg in HBV group was positive (Fig. 1B), but negative in the control group (Fig. 1A). Besides, the probe of HBV-DNA in HBV group was positive (Fig. 1D), but negative in the control group (Fig. 1C).

Differential expression analysis of transcriptome profiling

Furthermore, the transcriptome differences between the two groups (HBV vs Control) were detected. The original raw data of transcriptome sequencing were firstly obtained (Table 1), then data quality preprocessing was performed. There were three steps in quality preprocessing: 1) the proportional threshold was 50%, and the quality threshold was 20 (error rate = 1%), to remove low-quality reads; 2) cut N parts of the reads; 3) perform elimination of low-quality data at the end of the sequence. The results after

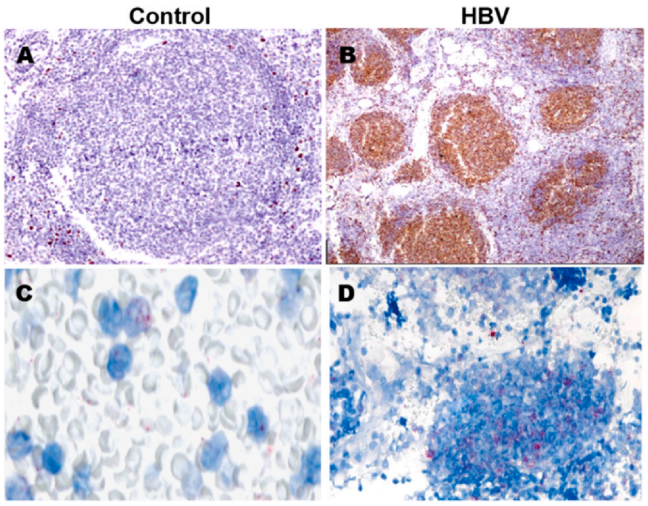

Fig. 1. The detection of HBV marker. The immunohistochemical stain of HBsAg in HBV group was positive (B), but negative in control group (A). Besides, the probe of HBV-DNA in HBV group was positive (D), but negative in control group (C).

Table 1
Raw sequencing data statistics for transcriptome.

Sample	Read length (R1; R2)	Sequencing Reads quantity	Total length of sequencing read (Gb)
Control	100;100	21,827,299	4.36
HBV	100;100	42,588,251	8.50

processing were shown in Table 2. Then, the statistics of gene mapping for transcriptome data was performed, too (Table 3). The mapped data of transcriptome and gene matched reads were shown in Table 4 and Table 5, respectively. Moreover, a random analysis of read length was conducted. Each gene sequence was extracted and checked the distribution of read length. Whether the random distribution of read lengths in transcripts of different samples was analyzed. The positional relationships of read lengths in transcripts over each transcript were counted. The areas were normalized to 0–100. Moreover, the random test of Kolmogorov-Smirnov test was used to check whether the position distribution of read length was uniformly distributed. P-value was greater than 0.05 indicating that the data did not show significantly different from the uniform distribution (Table 6).

From the above results, no significant difference between each read length and the uniform distribution was confirmed, so the uniformity of randomness was very fine, which met the expectations of the data analysis (Fig. 2). Furthermore, the differential genes expressions were analyzed that took genes as the unit and counted the expression abundance in different samples. Then the detections of DEGs (differentially expressed genes) from the two groups were conducted. The following informations were given separately as follows: Test_id: gene ID number; Locus: the location of gene in the chromosome; A: expression level of sample A (FPKM); B: expression level of sample B (FPKM); logFC: log multiple ratio; logCPM: the logarithmic sum of the expressed values; Pvalue: t-test significance level; FDR: the significance level of the FDR test gives the log odds ratio. We selected genes with P value < 0.05 and log2 (fold_change) > 1 as the screening conditions for conducting A-B comparative analysis of expression differences. Moreover, the GO classification analysis was performed. The results must meet two criteria: (1) the fold change is more than two times, which means logFC > 1; (2) $P < 0.05$. The differentially down-regulated and up-regulated gene of GO analysis was shown in Fig. 3A and Fig. 3B, respectively. Besides, the Kyoto Encyclopedia of Genes and Genomes (KEGG) analysis of metabolic pathways was also conducted. The upregulation pathway of axon guidance (Fig. 4A), oocyte meiosis (Fig. 4B), regulation of actin cytoskeleton (Fig. 4C), and viral myocarditis (Fig. 4D) was identified. Meanwhile, the downregulation of focal adhesion (Fig. 5A), hepatitis B (Fig. 5B), HTLV-1 infection (Fig. 5C), MAPK signaling pathway (Fig. 5D), osteoclast differentiation (Fig. 5E), p53 signaling pathway (Fig. 5F), pathways in cancer (Fig. 5G), PI3K-Akt signaling (Fig. 5H), proteoglycans in cancer (Fig. 5I), and salmonella infection (Fig. 5J) were obtained, respectively.

Table 2
Quality of pretreatment transcriptome data.

Sample	Raw data			Valid data			Valid Ratio (Read)
	Reads	N_base	Length	Reads	N_base	Length	
Control 1	42,588,251	14,276,600	101	26,253,644	0	25 −101	61.65%
Control 2	42,588,251	2797,900	101	24,741,808	0	25 −101	58.10%
HBV 1	21,827,299	6680,000	101	17,317,956	0	25 −101	79.34%
HBV 2	21,827,299	611,300	101	16,753,438	0	25 −101	76.75%

Table 3
The Statistics of Gene Mapping for transcriptome data.

Sample	Clean Reads	Gene Mapped Reads	Gene Mapped Ratio	Gene Unique Reads	Gene Unique Ratio
HBV	34,071,394	20,068,969	58.90%	10,953,790	54.58%
Control	52,507,288	31,012,192	59.06%	16,931,528	54.60%

Table 4
The mapped data of transcriptome.

Sample	Mapped Reads	Reads Perfact Match (%)	Reads 1 Mismatch	Reads 2 Mismatch	Reads Unique Count
HBV	20,068,969	15,075,202 (75.12%)	3200,529 (15.95%)	1793,238 (8.94%)	10,953,790 (54.58%)
Control	31,012,192	23,607,123 (76.12%)	4741,586 (15.29%)	2663,483 (8.59%)	16,931,528 (54.60%)

Table 5
The gene mapped data of transcriptome.

Sample	Reads Multi Pos	Gene Num	Gene MAX Mapped Reads	Gene Average Mapped Reads
HBV	9115,179 (45.42%)	29,573	390,597	678
Control	14,080,664 (45.40%)	29,769	771,586	1041

Table 6
Kolmogorov-Smirnov test for transcriptome data.

Sample	D value	P value
HBV	0.645	0.377
Control	0.633	0.400

Identification of circulating tumor cells (CTC)

The cancerous lesions can produce CTCs (Circulating tumor cells), which then enter the bloodstream [20]. It is considered that the metastasis precursors in various types of cancer are CTCs [21,22]. However, whether HBV drives their enhanced oncogenesis potential of lymphoma, especially for B-NHL.

Among the forty-one samples of HBV group, fifteen cases had twelve clusters of vimetin-positive cells, seventeen cases had double-positive (CK and Vimentin) stained cells (Fig. 6A), and the other eight cases had no positive detection. However, in the control group, seven cases had twelve clusters of vimetin-positive cells, six cases had double-positive (CK and Vimentin) stained cells (Fig. 6B), and the other twenty-three cases had no positive detection. It suggested the significantly difference between the two groups.

HBsAg significantly promoted lymphocytes associated with c-Myc and PD-L1

The previous investigation of our research group found that HBsAg significantly promoted the proliferation of human normal B lymphocyte line IM9. The results of the BrdU cell proliferation test indicated that the HBsAg protein significantly promoted the DNA synthesis of IM9. The results of the BrdU cell mitosis test suggested that HBsAg can significantly promote the mitosis of the human normal B lymphocyte line IM9. XTT test and CCK-8 test results also confirmed that HBsAg protein has a significant promoting effect on the cell proliferation IM9. However, its mechanism was unclear. Therefore, the transcriptome analysis was performed, and we found some novel clues. Furthermore, through culture of CTC, our results demonstrated that HBsAg protein significantly promoted the expression of c-Myc and PD-L1 in dose-dependent manner (Fig. 7A). However, when utilization of siRNA of c-Myc, both the expression of c-Myc and PD-L1 decreased indeed (Fig. 7B). It illustrated that the promoted effect induced by HBsAg in lymphcytes was associated with PD-L1 mediated by c-Myc.

Furthermore, the results of animal experiment accounted for HBV infection in HBV transgenic mice, xenograft model caused significantly tumor proliferation than that in the control group. Meanwhile, both the expression of c-Myc and PD-L1 increased surely (Fig. 7**C**).

Discussion

NHL (Non-hodgkin lymphoma) accounts for about 90% of lymphomas, the incidence of NHL is increasing rapidly and is harmful to human health, and its prognosis is extremely poor. Recent studies on the pathogenesis of B-cell lymphoma suggest that a B-cell subtype has been found in the germinal center. The proto-oncogene c-Myc in this subtype cell is highly activated, and c-Myc regulates key regulatory factor of cell proliferation. When the immune system encounters an infection, the germinal centers in the lymphatic system organs will produce a large number of B cells. These cells produce special antibodies against pathogens through changes in

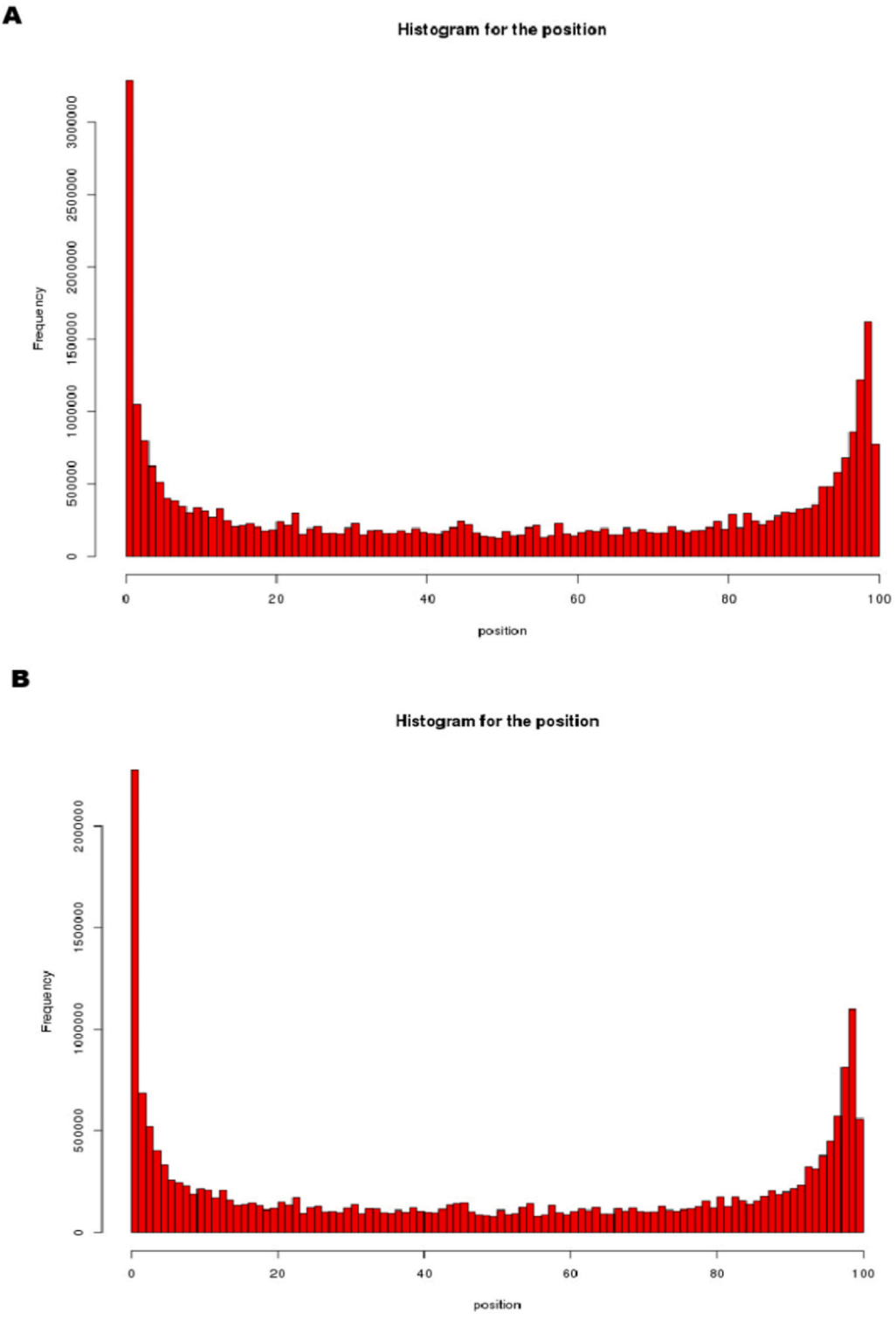

Fig. 2. The distribution of each read length and the uniform distribution. From the above results, we could see that there was no significant difference between the distribution of each read length and the uniform distribution, so the uniformity of randomness was very good, which met the expectations of the data analysis. (A) Control; (B) HBV.

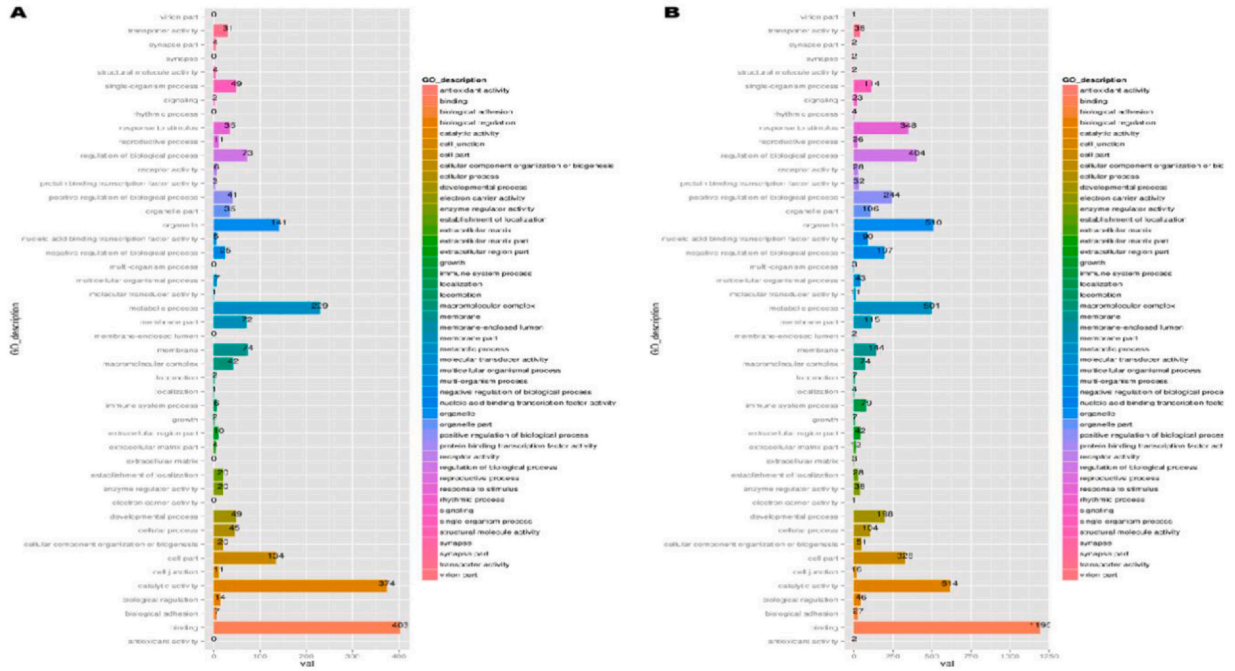

Fig. 3. The GO classification analysis. The GO classification analysis was performed. The results must meet two criteria: (1) the fold change is more than 2 times, which means logFC| > 1; (2) $P < 0.05$. The differentially up-regulated gene and down-regulated gene of GO analysis was shown in A and B, respectively.

their own DNA. However, the study also proved that this type of germinal center is also the source of most B-cell lymphomas, and the c-Myc gene in these cells plays an irreplaceable role in the formation and maintenance of germinal centers, which reveals the germinal center response origin of B-cell lymphoma [23].

C-Myc gene is a key regulatory gene for cell proliferation and is often associated with the chromosomal translocation of lymphoma whose germinal centers are derived from B cells. This translocation occurs in approximately 10% of DLBCL and almost all sporadic BL and c-Myc and its enhancers appear side by side at immunoglobulin sites, resulting in decreased c-Myc gene expression. Meanwhile, rapid proliferation and continuous DNA mutations may increase the occurrence of mutations and recombination errors, leading to malignant transformation of germinal center B cells. Most of B-cell lymphomas located in the germinal center that have undergone germinal center reactions. They found a type of B cell subgroup located in the germinal center. In these subgroups, the c-Myc gene is highly active. The researchers also discovered that c-Myc is an essential element for the formation and maintenance of the germinal center. When they knock out the c-Myc gene in B cells, the germinal center cannot be formed or maintained. C-Myc-positive germinal center B cell subsets may have high-risk malignant transformation. Their research directly affected scientists' understanding of the pathological process of human germinal center-derived B-cell lymphomas with c-Myc gene chromosomal translocation. It will also help to better analyze how these lymphomas occur and develop [24].

Hepatitis B virus surface antigen proteins (MHBs) can affect a variety of cell signal transduction pathways, activate a variety of viruses and cell gene promoters, and have a wide range of transactivation effects. Some studies have shown that the target genes transactivated by MHBs are screened by suppression subtractive hybridization. The screened sequence contains genes closely related to tumorigenesis, such as c-Myc. The immunoblotting method is further used to verify the effect of MHBs on c-Myc gene upregulation expression, the results show that c-Myc is the target gene of MHBs transactivation [25].

The generation of tumor immune response is the result of the combined effect of the host's immune function status and tumor immunogens. Many immune cells and molecules are widely involved in the occurrence, development, angiogenesis, recurrence, and metastasis of tumors. T cell costimulatory molecule programmed death-1 ligand (PD-L1) binds to the receptor programmed death-1 (PD-1) expressed on the surface of T cells, transmit inhibitory signals, causing T cells to develop immune tolerance even when stimulated by tumor antigens. The PD-1/PD-L1 costimulatory pathway mainly transmits inhibitory signals, leading to suppression of the immune activation of naive T cells. Tumor cells inhibit the function of T cells and B cells by upregulating the expression of PD-L1 and binding to PD-1 expressed on tumor infiltrating lymphocytes, thereby mediating tumor immune escape and promoting tumor growth [26].

Because the mechanism of B-NHL is very complicated and there are many interference factors, blocking PD-1/PD-L1 with antagonistic antibody or activating positive regulatory molecules with agnistic molecules (such as agnistic antibody to 4–1BB) to antagonize negative regulatory molecules, both of them are effective strategies for B-NHL treatment research. Clinical trial studies have confirmed that the PD-L1 antibody is effective in treating a variety of tumors, and the biomarker data suggests that the expression of PD-L1 in the tumor may be related to the antitumor effect of the PD-L1 antibody. In addition, there are preliminary data from many related studies suggesting that this targeted treatment is very promising [27].

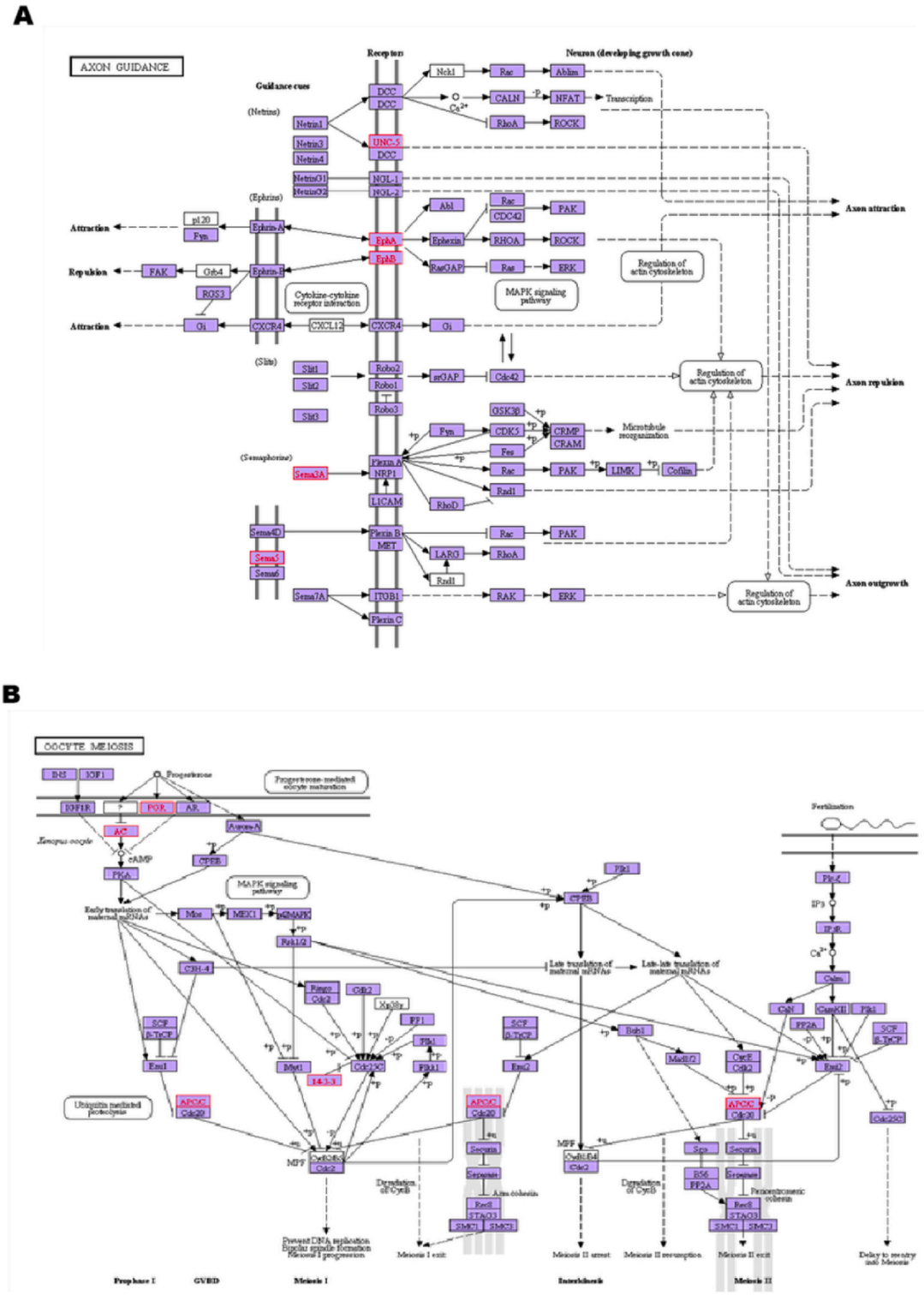

Fig. 4. KEGG (Kyoto Encyclopedia of Genes and Genomes) analysis of up-regulation metabolic pathways. KEGG (Kyoto Encyclopedia of Genes and Genomes) analysis of metabolic pathways was also conducted. The up-regulation pathways of axon guidance (A), oocyte meiosis (B), regulation of actin cytoskeleton (C), and viral myocarditis (D) was found.

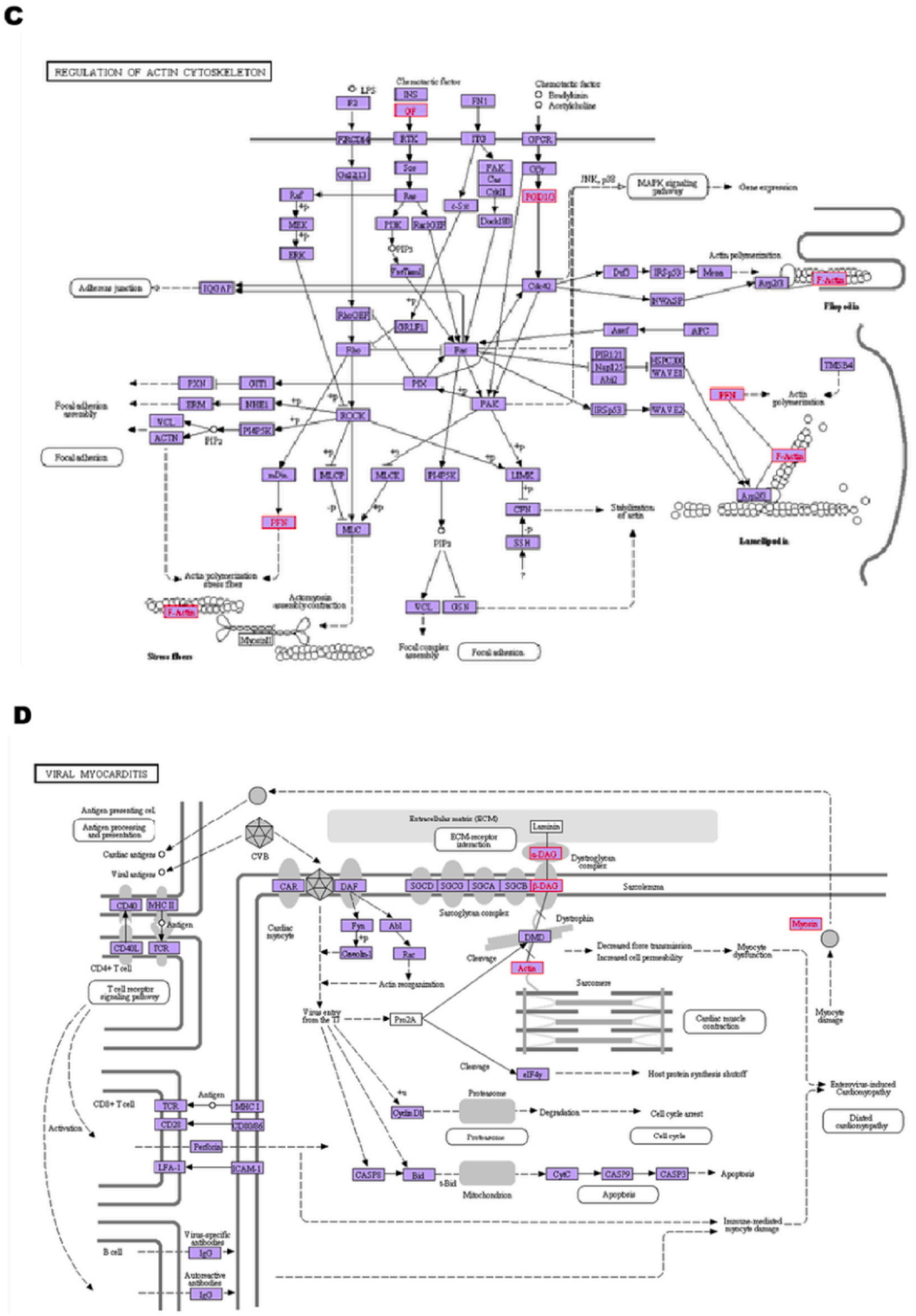

Fig. 4. (*continued*)

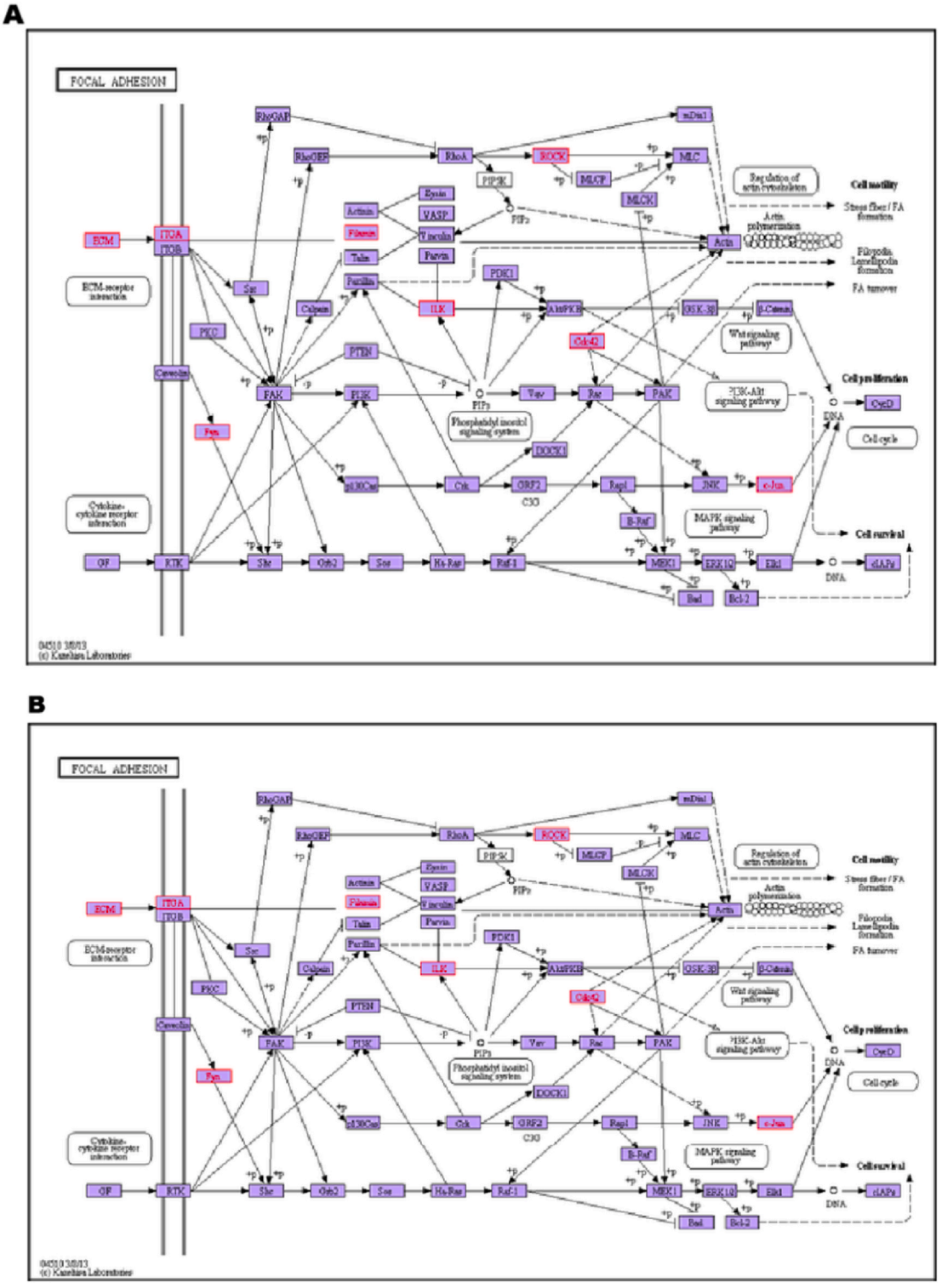

Fig. 5. KEGG (Kyoto Encyclopedia of Genes and Genomes) analysis of down-regulation metabolic pathways. Meanwhile, the down-regulation of focal adhesion (A), hepatitis B (B), HTLV-1 infection (C), MAPK signaling pathway (D), osteoclast differentiation (E), p53 signaling pathway (F), pathways in cancer (G), PI3K-Akt signaling (H), proteoglycans in cancer (I), and salmonella infection (J) were obtained, respectively.

C

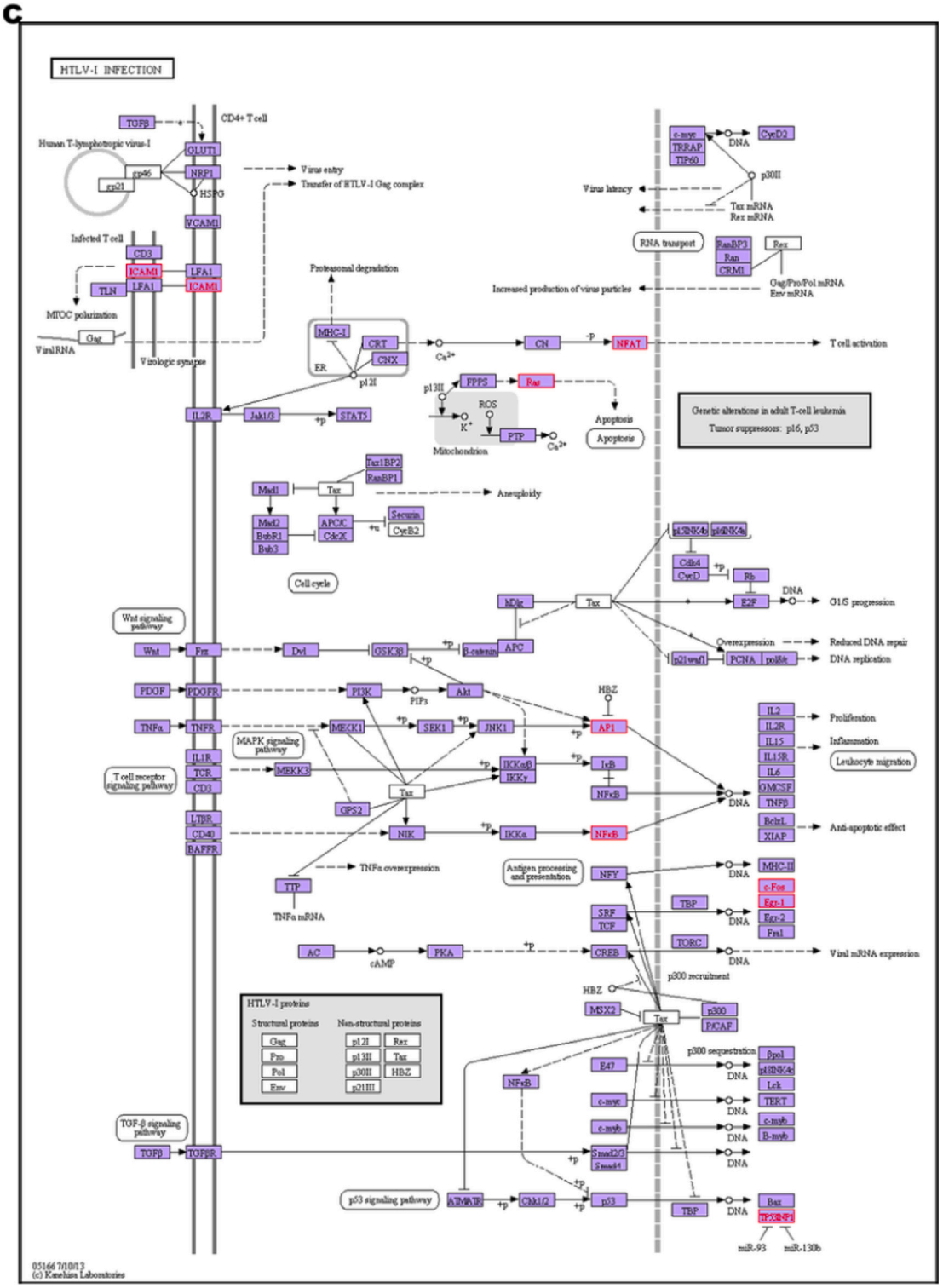

Fig. 5. (*continued*)

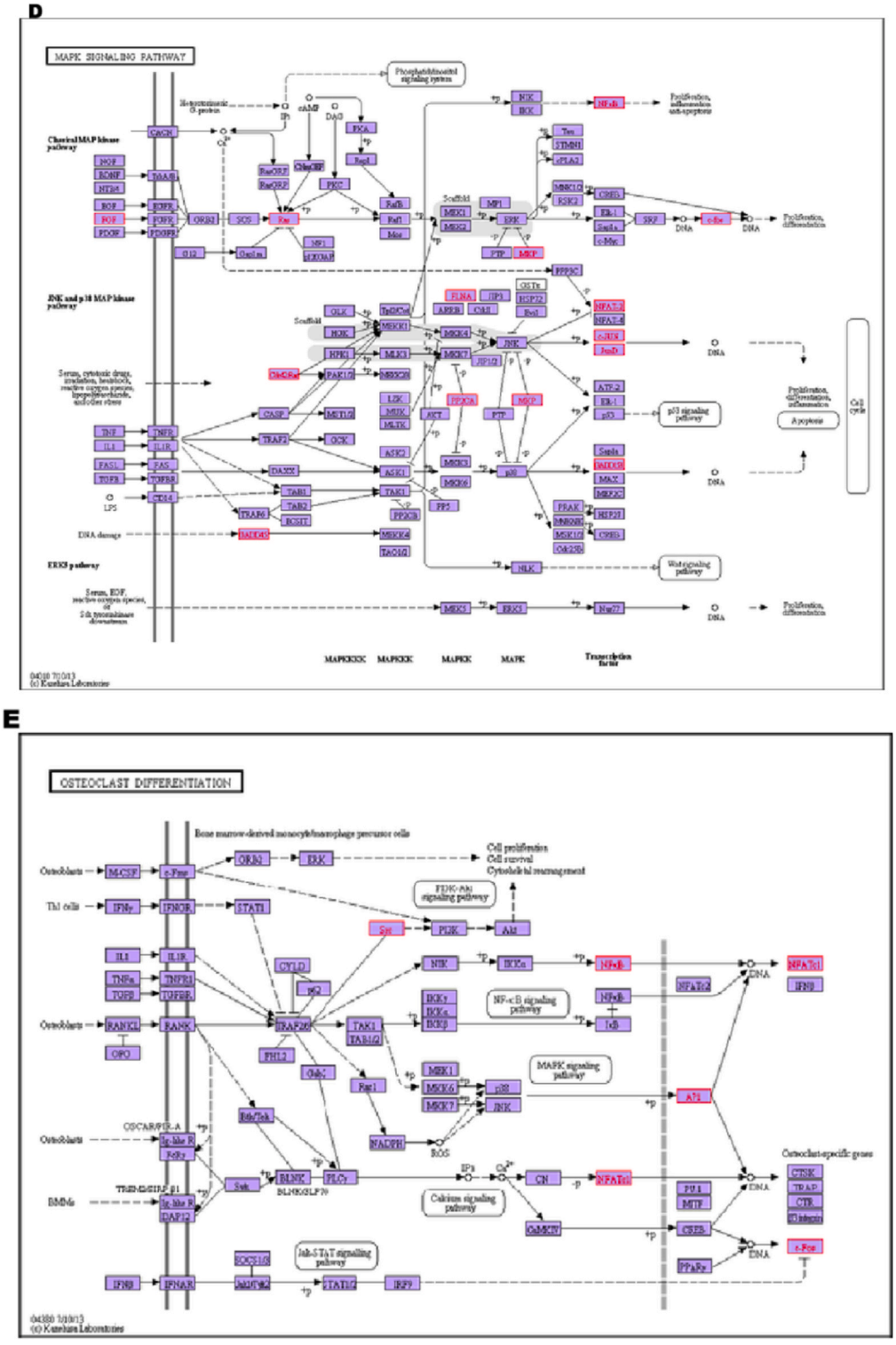

Fig. 5. (*continued*)

F

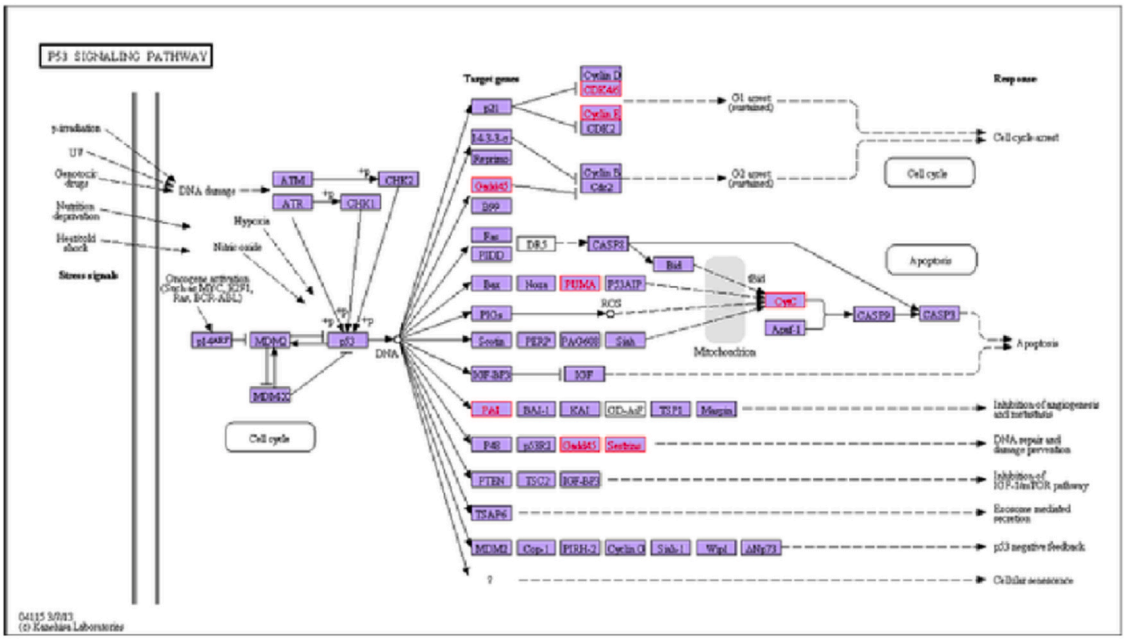

G

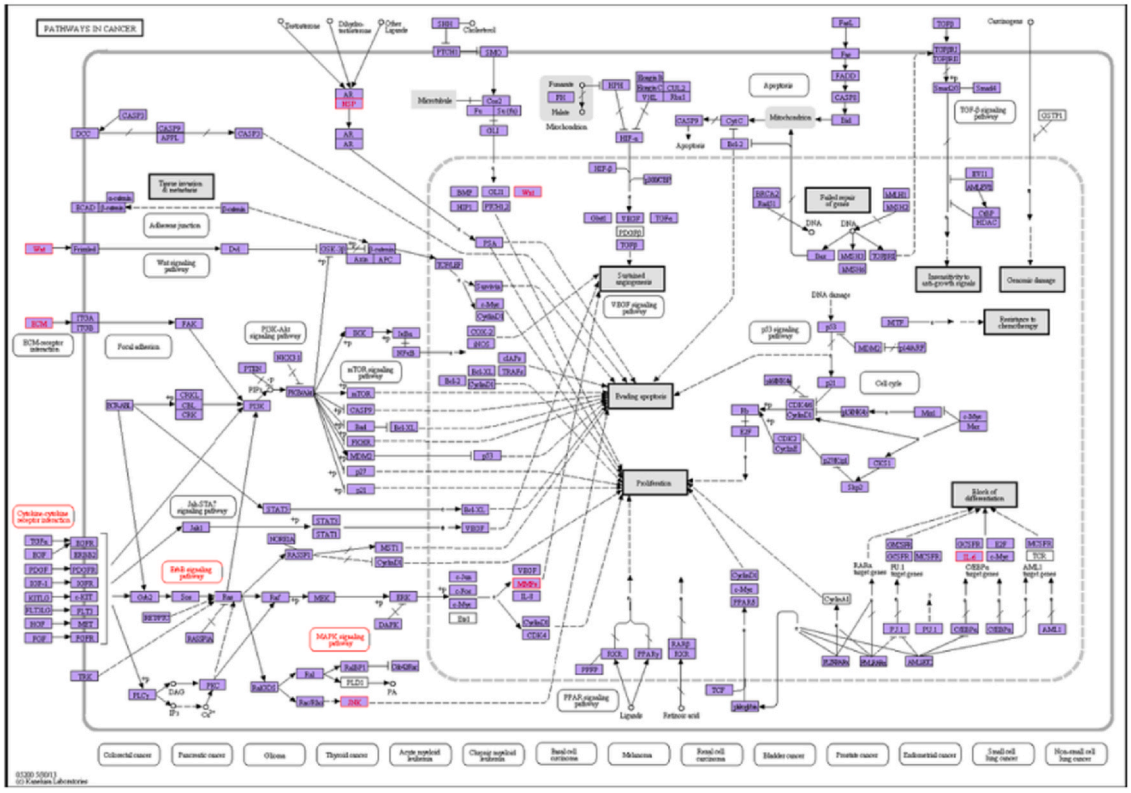

Fig. 5. (*continued*)

H

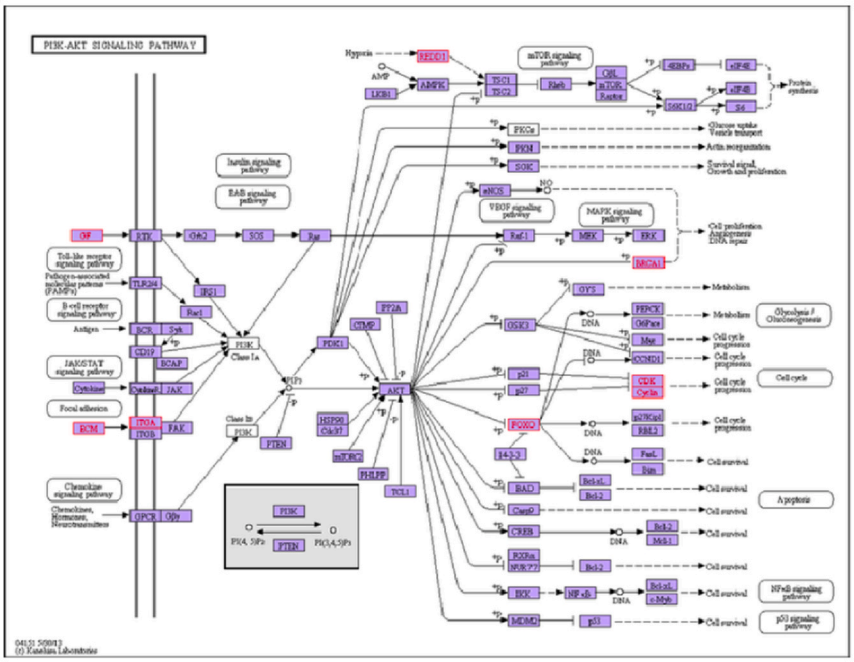

I

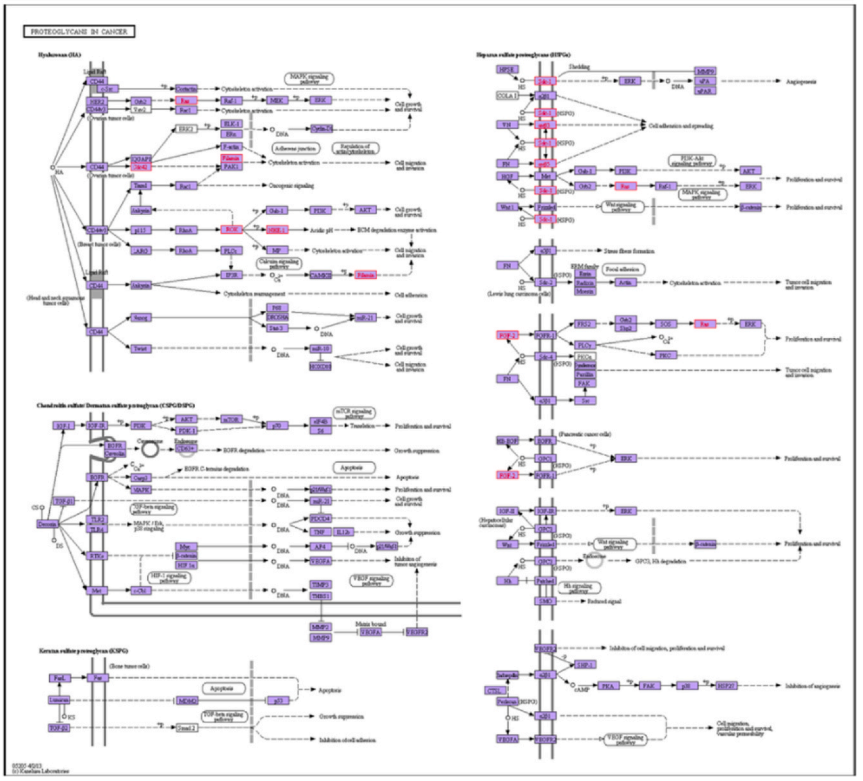

Fig. 5. (*continued*)

J

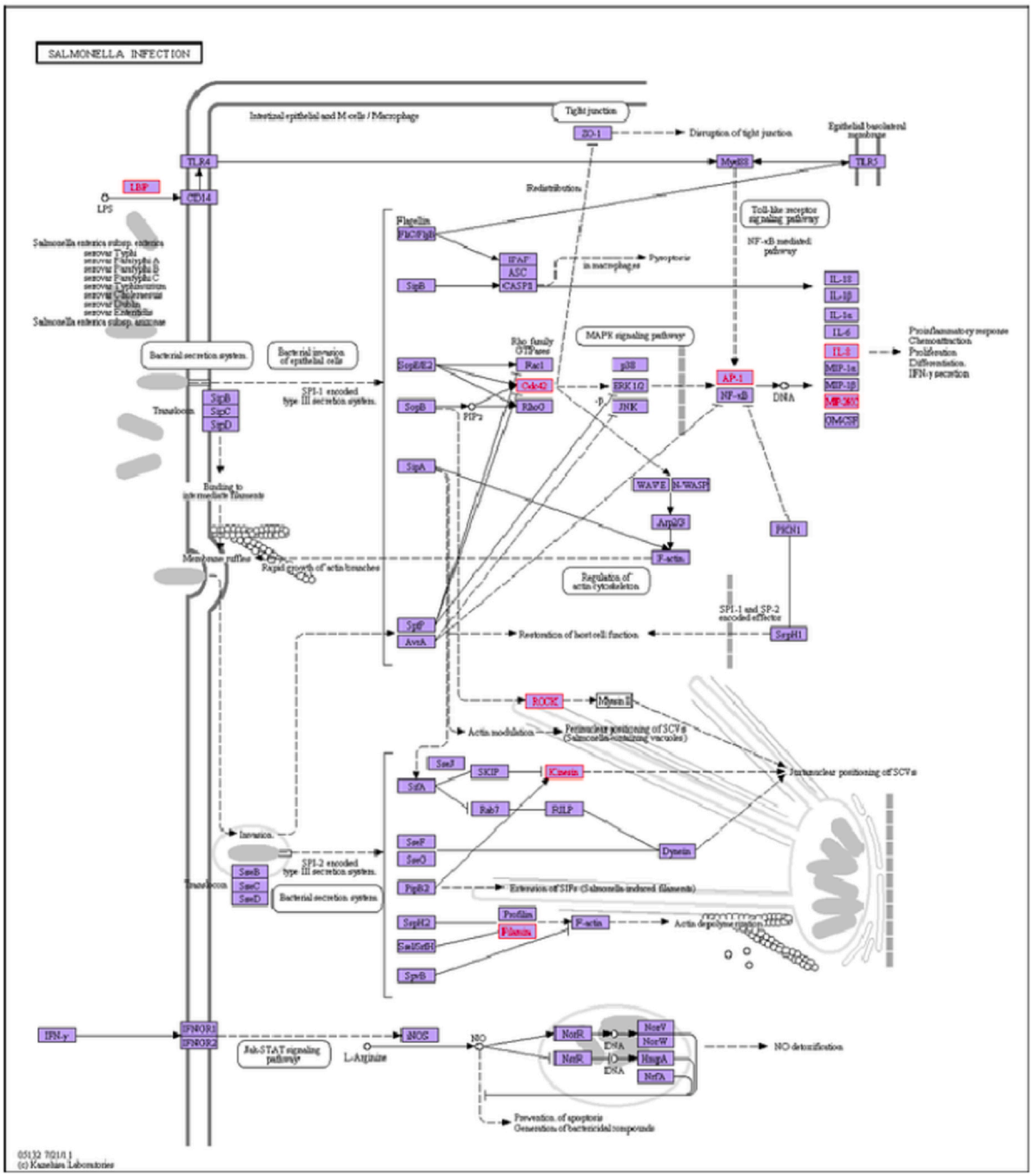

Fig. 5. (*continued*)

However, although the efficacy of PD-L1 antibody has improved compared with the original drugs, it is still limited. Currently, it is only effective for a small number of cancer patients. Moreover, the research of such drugs faces many tests: (1) whether the therapeutic effect is durable; (2) whether the combination of drugs improves the prognosis (because in general, combination therapy is more effective than any single therapy). The most important thing is that a large number of current studies clearly indicate that PD-L1 is closely related to B-NHL, but there is still no research report on PD-L1 antibody treatment of B-NHL [28].

The results of the previous research work of this group suggested that the expression level of PD-L1 protein in tumor tissues of B-NHL patients is significantly higher than that of adjacent tissues and normal lymph node tissues. Therefore, we believed that the expression of PD-L1 molecules in B-NHL might inhibit the function of T cells in B-NHL tissues and promote tumor cells to evade

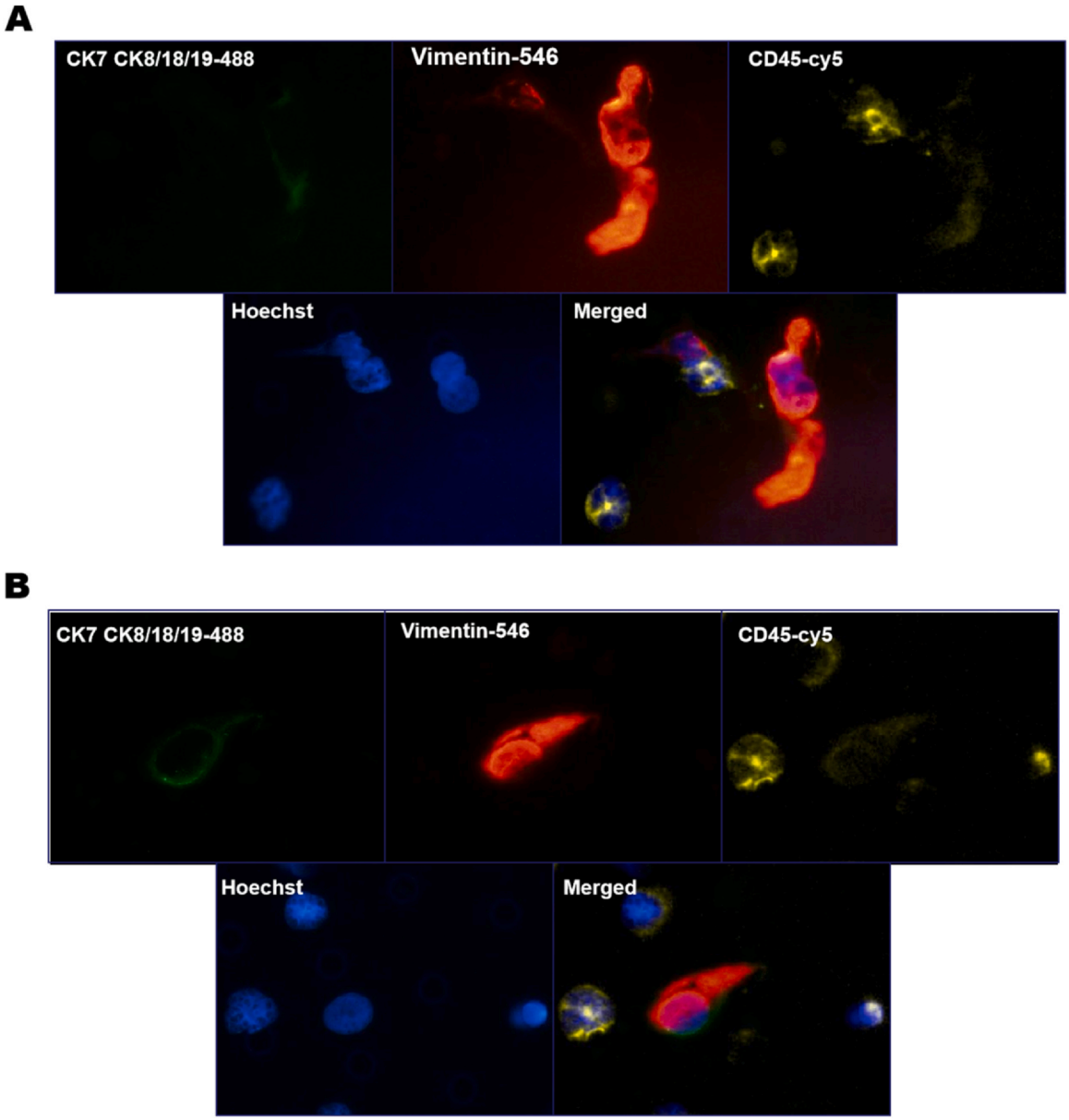

Fig. 6. Identification of circulating tumor cell (CTC). Among the forty-one samples of HBV group, fifteen case had twelve clusters of Vimetin-positive cells, seventeen case had double-positive (CK and Vimentin) stained cells (A), and the other eight cases had no positive detection. But in the control group, seven case had twelve clusters of Vimetin-positive cells, six case had double-positive (CK and Vimentin) stained cells (B), and the other twenty-three cases had no positive detection.

immune surveillance through blocking PD-1/PD-L1 signal transduction on the surface of tumor cells might become a novel immunotherapy approach for B-NHL. Hence, we chose to block the PD-1/PD-L1 pathway as one of the research goals and use the inhibition of PD-L1 expression in B-NHL tumor cells as the research target.

In a great deal of human tumors, the oncogene MYC is overexpressed to encode its transcription factors. Some studies have confirmed MYC regulates two immune checkpoint protein expression on the surface of cancer cells, CD47 and programmed death ligand 1 (PD-L1). Inhibition of MYC in cancer cells resulted in a decrease of mRNA and protein levels of CD47 and PD-L1. The study confirmed that MYC could directly bind to the PD-1 and CD47 genes promoter areas. MYC inactivation could downregulated PD-L1 and CD 47 expression, then promote antitumor immune response. Conversely, while inactivated MYC would increase PD-L1 and CD47 expression causing the suppression of the immune response, and consequently the continuing tumor grow. Therefore, MYC may initiate and maintain tumorigenesis in part by regulating immunomodulatory molecules [29].

The previous research of our group has found that in the tumor tissues of HBsAg-positive patients with B-NHL, HBsAg expression could be detected based on immunohistochemistry analysis, meanwhile HBV-DNA was positive according to situ hybridization. Additionally, HBsAg protein can significantly upregulate the expression level of c-Myc and PD-L1 in normal human B lymph nodes,

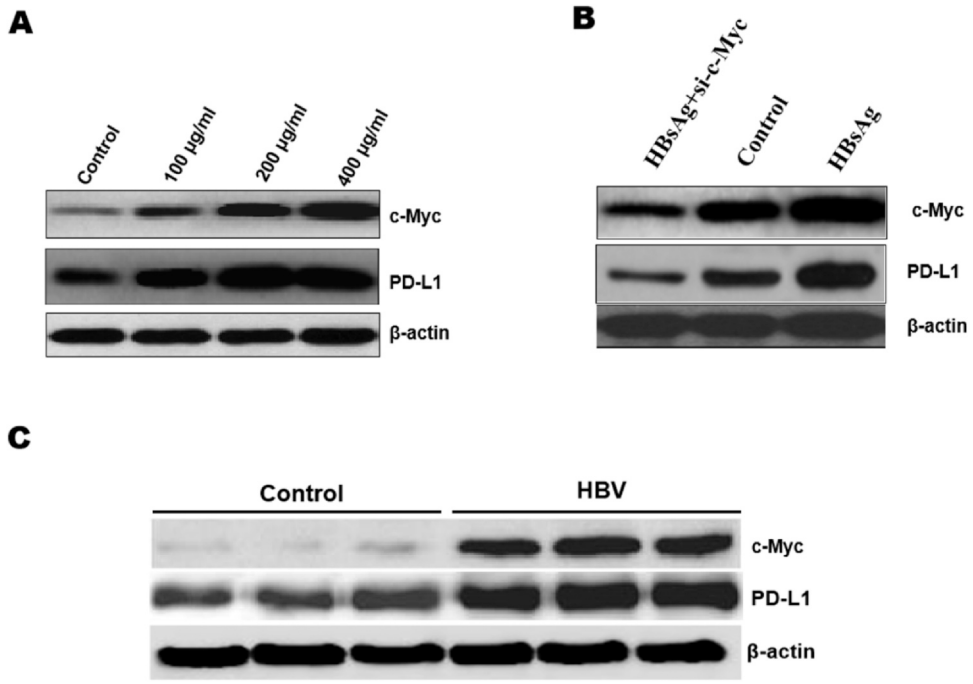

Fig. 7. HBsAg protein significantly promoted the expression of c-Myc and PD-L1. Through culture of CTC, our results demonstrated that HBsAg protein significantly promoted the expression of c-Myc and PD-L1 with dose-dependent manner (A). But when utilization of siRNA of c-Myc, both the expression of c-Myc and PD-L1 decreased obviously (B). Furthermore, the results of animal experiment accounted for HBV infection in HBV transgenic mice xenograft model caused significantly the tumor proliferation than that in the control group. Meanwhile, both the expression of c-Myc and PD-L1 increased obviously (C).

and promote cell proliferation. Therefore, this project intended to establish the cell and animal model of B-NHL caused by HBV infection to clarify the interaction between the HBV infection process and the pathogenesis of B-NHL. Furthermore, our work explored and determined that HBsAg protein was regulated by c-Myc during the process of B-NHL caused by HBV infection associated with PD-L1 signaling pathway.

In this work, the relationship between HBV and B-NHL was studied based on the HBV infection model, which included CTC cells and HBV transgenic mice. Moreover, differential expression analysis of transcriptome profiling was performed to confirm the mechanism. Our results declared that the HBsAg expression and HBV-DNA could be found in tumor tissues of HBV group, but negative in the control group. There were clearly differences between the two groups in the transcriptome of tumor tissues and CTC. HBsAg significantly promoted lymphocytes associated with c-Myc and PD-L1. In conclusion, the promoted effect induced by HBsAg in lymphcytes was associated with PD-L1 mediated by c-Myc.

If the same problems occur and are inevitable in all studies, our work also has many shortcomings. This study only refined the KEGG pathway analysis, but not further focused on specific enriched pathways rather than displaying entire pathways. Therefore, in the next step, we will delve deeper into analyzing the key signaling pathways at the core of HBV associated B-NHL related to PD-L1 mediated by c-Myc. To optimize this aspect for greater accuracy and clarity. Besides, due to the current level and status of research, we are unable to fully simulate the pathophysiological process of B-NHL in humans after HBV infection, which makes it even more difficult to explore its key pathogenesis. Consequently, it should develop effective animal models, such as using organoids, to study the mechanisms of related diseases.

Funding

Hainan Natural Science Foundation of China (No. 817351).

Declaration of Competing Interest

The authors declare that there is no conflict of interest.

Acknowledgements

None.

References

[1] K.R. Shankland, J.O. Armitage, B.W. Hancock, Non-Hodgkin lymphoma, Lancet 380 (2012) 848–857.
[2] D.A. Arber, A. Orazi, R. Hasserjian, J. Thiele, M.J. Borowitz, M.M. Le Beau, C.D. Bloomfield, M. Cazzola, J.W. Vardiman, The 2016 revision to the World Health Organization classification of myeloid neoplasms and acute leukemia, Blood 127 (2016) 2391–2405.
[3] D.A. Eichenauer, I. Becker, I. Monsef, N. Chadwick, V. de Sanctis, M. Federico, C. Fortpied, A.M. Gianni, M. Henry-Amar, P. Hoskin, P. Johnson, S. Luminari, M. Bellei, A. Pulsoni, M.R. Sydes, P. Valagussa, S. Viviani, A. Engert, J. Franklin, Secondary malignant neoplasms, progression-free survival and overall survival in patients treated for Hodgkin lymphoma: a systematic review and meta-analysis of randomized clinical trials, Haematologica 102 (2017) 1748–1757.
[4] E.S. Jaffe, Diagnosis and classification of lymphoma: impact of technical advances, Semin. Hematol. 56 (2019) 30–36.
[5] K. Basso, R. Dalla-Favera, Germinal centres and B cell lymphomagenesis, Nat. Rev. Immunol. 15 (2015) 172–184.
[6] R. Küppers, Mechanisms of B-cell lymphoma pathogenesis, Nat. Rev. Cancer 5 (2005) 251–262.
[7] B.C. Chiu, N. Hou, Epidemiology and etiology of non-hodgkin lymphoma, Cancer Treat. Res. 165 (2015) 1–25.
[8] C.E. Huang, Y.H. Yang, Y.Y. Chen, J.J. Chang, K.J. Chen, C.H. Lu, K.D. Lee, P.C. Chen, C.C. Chen, The impact of hepatitis B virus infection and vaccination on the development of non-Hodgkin lymphoma, J. Viral Hepat. 24 (2017) 885–894.
[9] M. Li, Y. Gan, C. Fan, H. Yuan, X. Zhang, Y. Shen, Q. Wang, Z. Meng, D. Xu, H. Tu, Hepatitis B virus and risk of non-Hodgkin lymphoma: an updated meta-analysis of 58 studies, J. Viral. Hepat. 25 (2018) 894–903.
[10] T. Tian, C. Song, L. Jiang, J. Dai, Y. Lin, X. Xu, C. Yu, Z. Ge, Y. Ding, Y. Wen, B. Liu, Y. Shao, P. Shi, C. Zhu, Y. Liu, S. Jing, Z. Wang, Z. Hu, J. Li, Hepatitis B virus infection and the risk of cancer among the Chinese population, Int. J. Cancer 147 (2020) 3075–3084.
[11] M. Lemaitre, P. Brice, M. Frigeni, O. Hermine, L. Arcaini, C. Thieblemont, C. Besson, Hepatitis B virus-associated B-cell non-Hodgkin lymphoma in non-endemic areas in Western Europe: clinical characteristics and prognosis, J. Infect. 80 (2020) 219–224.
[12] X. Zhou, P. Wuchter, G. Egerer, M. Kriegsmann, F.K.F. Kommoss, M. Witzens-Harig, K. Kriegsmann, Serological hepatitis B virus (HBV) activity in patients with HBV infection and B-cell non-Hodgkin's lymphoma, Eur. J. Haematol. 104 (5) (2020) 469–475.
[13] M. Li, Y. Shen, Y. Chen, H. Gao, J. Zhou, Q. Wang, C. Fan, W. Zhang, J. Li, H. Cong, J. Gu, Y. Gan, H. Tu, Characterization of hepatitis B virus infection and viral DNA integration in non-Hodgkin lymphoma, Int. J. Cancer 147 (2020) 2199–2209.
[14] X. Zhou, H. Pan, P. Yang, P. Ye, H. Cao, H. Zhou, Both chronic HBV infection and naturally acquired HBV immunity confer increased risks of B-cell non-Hodgkin lymphoma, BMC Cancer 19 (2019) 477.
[15] S. Chiatamone Ranieri, M.A. Arleo, S. Trasarti, L. Bizzoni, I. Carmosino, M.L. De Luca, S. Mohamed, E. Mariggiò, E. Scalzulli, S. Rosati, D. De Benedittis, G. Colafigli, S. Pepe, M. Molica, M.C. Scamuffa, A. Di Prima, A. Ferretti, E. Baldacci, M. Mancini, C. Santoro, M. Vignetti, M. Breccia, R. Latagliata, Clinical and prognostic features of essential thrombocythemia: comparison of 2001 WHO versus 2008/2016 WHO criteria in a large single-center cohort, Clin. Lymphoma Myeloma Leuk. 21 (2021) e328–e333.
[16] S.H. Swerdlow, E. Campo, S.A. Pileri, N.L. Harris, H. Stein, R. Siebert, R. Advani, M. Ghielmini, G.A. Salles, A.D. Zelenetz, E.S. Jaffe, The 2016 revision of the World Health Organization classification of lymphoid neoplasms, Blood 127 (2016) 2375–2390.
[17] F.V. Chisari, C.A. Pinkert, D.R. Milich, P. Fillipi, A. McLachian, R.D. Palmiter, R.L. Brinster, A transgenic mouse model of the chronichepatitis B surface antigen carrier state, Science 230 (1985) 1157–1160.
[18] F.V. Chisari, P. Filippi, A. McLachian, D.R. Milich, M. Riggs, S. Lee, R.D. Palmiter, C.A. Pinkert, R.L. Brinster, Expression of hepatitis B virus large envelope polypeptide inhibits hepatitis B surface antigen secretion in transgenic mice, J Virol 60 (1986) 880–887.
[19] F.V. Chisari, P. Filippi, F. Buras, A. McLachian, H. Popper, C.A. Pinkert, R.D. Palmiter, R.F. Brinster, Structural and pathological effects of synthesis of hepatitis B virus large envelope polypeptide in transgenicmice, Proc. Nati. Acad. Sci. USA 84 (1987) 6909–6913.
[20] C. Alix-Panabières, K. Pantel, Circulating tumor cells: liquid biopsy of cancer, Clin. Chem. 59 (2013) 110–118.
[21] N. Aceto, M. Toner, S. Maheswaran, D.A. Haber, En route to metastasis: circulating tumor cell clusters and epithelial-to-mesenchymal transition, Trends Cancer 1 (2015) 44–52.
[22] C. Alix-Panabières, K. Pantel, Challenges in circulating tumour cell research, Nat. Rev. Cancer. 14 (2014) 623–631.
[23] D. Ennishi, A. Jiang, M. Boyle, B. Collinge, B.M. Grande, S. Ben-Neriah, C. Rushton, J. Tang, N. Thomas, G.W. Slack, P. Farinha, K. Takata, T. Miyata-Takata, J. Craig, A. Mottok, B. Meissner, S. Saberi, A. Bashashati, D. Villa, K.J. Savage, L.H. Sehn, R. Kridel, A.J. Mungall, M.A. Marra, S.P. Shah, C. Steidl, J.M. Connors, R.D. Gascoyne, R.D. Morin, D.W. Scott, Double-hit gene expression signature defines a distinct subgroup of germinal center B-cell-like diffuse large B-cell lymphoma, J. Clin. Oncol. 37 (2019) 190–201.
[24] D. Calado, Y. Sasaki, S. Godinho, et al., The cell-cycle regulator c-Myc is essential for the formation and maintenance of germinal centers, Nat. Immunol. 13 (2012) 1092–1100.
[25] Y.Z. Lun, J. Cheng, Q. Chi, X.L. Wang, M. Gao, L.D. Sun, Transactivation of proto-oncogene c-Myc by hepatitis B virus transactivator MHBst167, Oncol. Lett. 8 (2014) 803–808.
[26] D. Escors, M. Gato-Cañas, M. Zuazo, et al., The intracellular signalosome of PD-L1 in cancer cells, Sig Transduct. Target. Ther. 3 (2018) 26.
[27] W.Y. Lai, B.T. Huang, J.W. Wang, P.Y. Lin, P.C. Yang, A novel PD-L1-targeting antagonistic DNA aptamer with antitumor effects, Mol. Ther. Nucleic Acids 5 (2016) e397.
[28] P. Tan, L. He, C. Xing, J. Mao, X. Yu, M. Zhu, L. Diao, L. Han, Y. Zhou, M.J. You, H.Y. Wang, R.F. Wang, Myeloid loss of Beclin 1 promotes PD-L1hi precursor B cell lymphoma development, J. Clin. Invest. 129 (2019) 5261–5277.
[29] S.C. Casey, L. Tong, Y. Li, R. Do, S. Walz, K.N. Fitzgerald, A.M. Gouw, V. Baylot, I. Gütgemann, M. Eilers, D.W. Felsher, MYC regulates the antitumor immune response through CD47 and PD-L1, Science 352 (2016) 227–231.